Eur. Phys. J. B **79**, 465–471 (2011)
DOI: 10.1140/epjb/e2011-10875-9

THE EUROPEAN PHYSICAL JOURNAL B

Regular Article

Hatano-Nelson model with a periodic potential

F. Hébert[1,a], M. Schram[2], R.T. Scalettar[3], W.B. Chen[4], and Z. Bai[5]

[1] INLN, Université de Nice-Sophia Antipolis, CNRS, 1361 route des Lucioles, 06560 Valbonne, France
[2] Physics Department, Massachusetts Institute of Technology, 77 Massachusetts Avenue Cambridge, 02139-4307 MA, USA
[3] Physics Department, University of California, Davis, 95616 California, USA
[4] School of Mathematical Sciences, Fudan University, Shanghai 200433, P.R. China
[5] Departments of Mathematics and Computer Science, University of California, Davis, 95616 California, USA

Received 14 November 2010 / Received in final form 11 January 2010
Published online 16 February 2011 – © EDP Sciences, Società Italiana di Fisica, Springer-Verlag 2011

Abstract. We study a generalisation of the Hatano-Nelson Hamiltonian in which a periodic modulation of the site energies is present in addition to the usual random distribution. The system can then become localized by disorder or develop a band gap, and the eigenspectrum shows a wide variety of topologies. We determine the phase diagram, and perform a finite size scaling analysis of the localization transition.

1 Introduction

The Anderson transition [1,2], in which eigenstates of non-interacting electrons are localized by disorder, has long been a paradigm of a metal-insulator transition in solid state physics. The metallic phase occurs only in three dimensions, since any amount of randomness localizes all particles in one or two dimensions. In three dimensions, a mobility edge separates localized states whose energies lie at the edges of the spectrum, from extended states whose energies lie in the middle. The mobility edges appear for a critical value of the disorder and move with the disorder until no extended states remain. If the Fermi energy is located below or above the mobility edge, inside the localized states, the system is then an insulator. Recently, research on this subject has experienced renewed interest as localization of cold atoms in the presence of a disordered optical potential has been observed [3,4]. Whereas experiments in solid state physics are intrinsically limited as interactions between electrons cannot be neglected, cold atoms allow the exploration of the non-interacting regimes with possibilities of control that could not be achieved before.

Another, simpler origin for an insulating behavior in a solid is the presence of gaps due to a periodic potential applied to the particles. These two possible insulating phases are in competition with each other as they are based on opposite behaviors. The Anderson insulator is due to the localized nature of the wave function, whereas the gapped insulator is due to its extended nature. A third source of insulating behavior is interactions between particles. In many ways this is the most difficult situation, since it involves treating the many-body problem accurately. In the systems with both interactions and randomness, competition between Mott and band insulating phases have been shown to result in metallic phases, as the two sources of insulating behavior counteract each other [5,6]. The possibility of metallic phases arising due to the addition of interactions to two dimensional disordered systems has also been an area of great interest [7–9].

The goal of this article is to study the interplay between the two sources of single particle insulating behavior- disorder and gaps due to a periodic potential- in the context of non-Hermitian matrices. For this we will use a modified version of the Hatano-Nelson model (HNM), that includes at the same time a periodic potential that generates gaps in the eigenspectrum and a disordered potential that will drive a localization transition. The HNM [10,11] is a single particle, random, non-Hermitian Hamiltonian that was introduced to study the motion of magnetic flux lines in disordered type II superconductors, the path integral representation of the HNM being analogous to a classical model used to describe the flux lines. The HNM shows a localization transition in one dimension [10–13]. It is then a very convenient tool to study the localization transition numerically, as it allows the study of systems with large linear sizes.

The paper is organised as follows. In Section 2 we introduce the HNM and recall some basic properties. In Section 3, we present the different regimes which can be observed. Section 4 contains a detailed analysis of some of the transitions appearing in the generalized HNM. The conclusion describes some of the connections the additional term we introduce into the Hatano-Nelson model has with the eigenspectrum of several physical systems for whose properties random matrices have been used.

[a] e-mail: frederic.hebert@inln.cnrs.fr

2 Modified Hatano-Nelson model

2.1 Hatano-Nelson model

The Hatano-Nelson model is a discrete model similar to the Anderson model used to study localization. In one dimension,

$$\mathcal{H}_{\rm HN} = \sum_{x=1}^{L} \left[-\frac{t}{2} \left(e^{h} c_{x+1}^{\dagger} c_x + e^{-h} c_x^{\dagger} c_{x+1} \right) + \mu_x n_x \right] \quad (1)$$

here $c_x^{\dagger}(c_x)$ are the usual fermionic creation (destruction) operators and $n_x = c_x^{\dagger} c_x$ is the number of particles on site x. The first term of the Hamiltonian describes the hopping of particles between sites, and the parameter h controls the asymmetry between the hopping amplitudes in the left and right directions. We will choose the random sites energies μ_x according to a uniform distribution on the interval $[-\Delta/2, +\Delta/2]$. The hopping parameter t is set to one to fix the energy scale and L is the number of lattice sites.

In the absence of disorder ($\Delta = 0$) the eigenenergies are given by,

$$\epsilon_k = \frac{t}{2} \left(e^{h + ik\,2\pi/L} + e^{-h - ik\,2\pi/L} \right) \quad (2)$$

where $k = 1, 2 \ldots L$. All the eigenvalues (except $k = L/2, L$) are complex and lie on an ellipse in the complex plane, centered at the origin. When disorder is turned on, $\Delta \neq 0$, the eigenvalues of the $d = 1$ HNM remain confined to one dimensional curves in the complex plane [14], however, some of the eigenvalues become real. The corresponding eigenstates become localized (Fig. 1). We will continue to use the notation ϵ_k for the eigenvalues for nonzero Δ even though momentum is no longer a good quantum number due to the breaking of translation invariance by the disorder. k will be understood to be a generic mode label.

One way to understand the appearance of real eigenvalues is to consider a system with open boundary conditions (OBC) [10,11]. In this case, all the eigenvalues of $\mathcal{H}_{\rm HN}$ are real, despite the fact that the Hamiltonian is not Hermitian. In fact, the eigenspectrum is independent of h, since the $e^{\pm h}$ factors can be "gauged away" by a suitable redefinition $\tilde{\phi}(x) = e^{-hx}\phi(x)$, of the eigenvector components. The HNM spectrum becomes identical to that of the Anderson model. On a system with periodic boundary conditions (PBC), however, this eigenvector transformation is no longer possible, and some eigenvalues are complex (see Fig. 1).

The dramatic difference in the spectrum between OBC and PBC of course reflects a rather general property of the localization transition: a localized state is insensitive to the boundary conditions and its eigenvalue should remain real, even in the presence of PBC. On the contrary, an extended state, for example a plane wave state, is sensitive to the boundary conditions and its eigenvalue should be complex in the PBC case (Fig. 1).

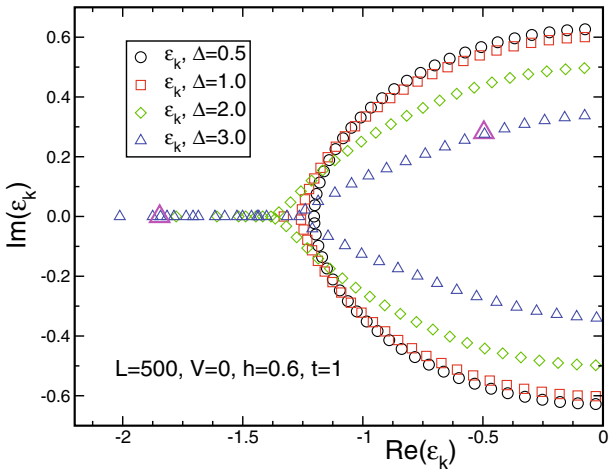

Fig. 1. (Color online) Typical spectra of the Nelson-Hatano model. In the presence of disorder, localized states (real eigenvalues) appear for Δ larger than a critical value. Half of the spectra are shown and the spectra are approximately symmetric around the imaginary axis. The two larger up triangles correspond to the eigenstates used for Figure 2.

Le Doussal [15] has further clarified the relation between the eigenvector tranformation and the localization length by pointing out that the eigenvalues will remain real if the localization decay $e^{-l/\xi}$ is more rapid than the growth e^{hl} induced by the transformation. As a consequence, the localization length ξ does not diverge at the transition, but takes on the value $\xi = 1/h$ at the bifurcation point in Figure 1 where the line of real eigenvalues splits off into the complex plane.

For the particular case of a Cauchy distribution of randomness, $P(\Delta) = \gamma/\pi(\gamma^2 + \Delta^2)$ the location of the bifurcation point is known [12] to be given by $\mathrm{Re}[\epsilon_k] = \sqrt{(2t \sinh h)^2 - \gamma^2}/\tanh h$, and $\mathrm{Re}[\epsilon_k] = 0$ at the critical value $\gamma_c = 2t\sinh h$. At this point the randomness is sufficiently large that all eigenvalues are real, and all modes are localized.

More direct evidence of the localized nature of the eigenstates with real eigenvalues can be obtained by directly looking at how the corresponding density varies with distance [12]. For example, we can study the participation ratio P_k for a given eigenvalue ϵ_k. As the Hatano-Nelson model is non-Hermitian, the left eigenvector $\langle k| = \sum_x \langle x|\phi_k^L(x)$ and right eigenvector $|k\rangle = \sum_x \phi_k^R(x)|x\rangle$ are not Hermitian conjugates. It was shown [12] that the probability density in these systems is given by $|\phi_k^L(x)\phi_k^R(x)|$ which is a better behaved quantity than $|\phi_k^L(x)|^2$ or $|\phi_k^R(x)|^2$ although they give quite similar results for localized states (Fig. 2).

Then the participation ratio P_k can be defined as,

$$P_k = \frac{1}{L} \sum_x \left| \phi_k^L(x) \phi_k^R(x) \right|^2 \quad (3)$$

P_k corresponds to the portion of the lattice sites that is occupied for a given eigenvalue. It goes to zero for a localized state in a large system and goes to a number of order

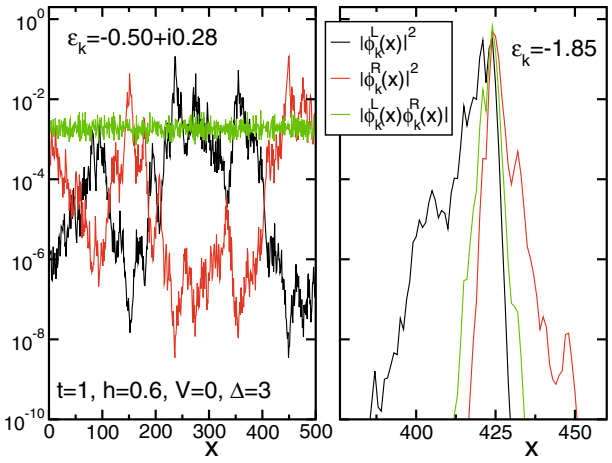

Fig. 2. (Color online) Three different possible definitions of the density in an extended (left) and localized (right) states corresponding to different eigenvalues ϵ_k of the same system. In general $|\phi_k^{L,R}(x)|^2$ show quite strong fluctuations, thus making $|\phi_k^L(x)\phi_k^R(x)|$ a better quantity to identify the different states.

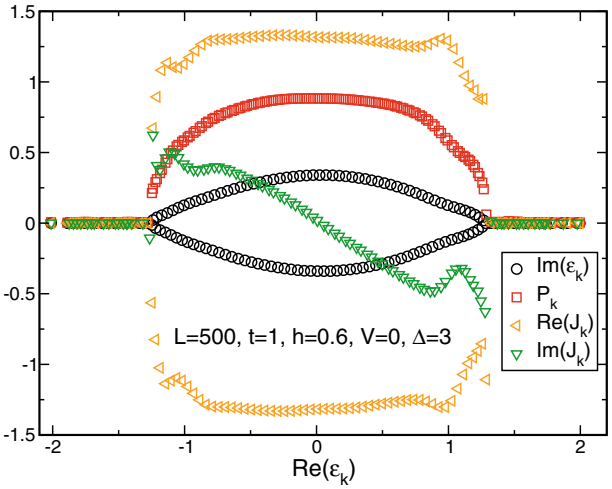

Fig. 3. (Color online) Different quantities which distinguish the extended from the localised states in the Hatano Nelson model: the imaginary part of the eigenvalues $\mathrm{Im}(\epsilon_k)$, participation ratio P_k, and real $\mathrm{Re}(J_k)$ and imaginary $\mathrm{Im}(J_k)$ parts of the current. All these quantities give consistent information concerning which modes are localized or not.

unity for an extended state when the density distribution is spread equally over all the sites. Figure 3 shows that the vanishing of the participation ratio aligns nicely with the energy at which the eigenvalues are real. Similar participation ratios can be defined with other definitions of the density $P_k^{L,R} = \sum_x |\phi_k^{L,R}(x)|^2/L$. But, as for the densities (Fig. 2) themselves, P_k is better behaved than $P_k^{L,R}$.

The current J_k defined as $J_k = -i\partial\epsilon_k/\partial h$ [11] is compared with the participation ratio in Figure 3. It gives similar results for the extended or localized nature of the states, but is more difficult to calculate as it requires a numerical derivative (and then two diagonalization instead of one for the participation ratios) and is difficult to define close to the mobility edges.

2.2 Effect of a periodic potential

Our interest here is in adding a simple potential of period 2 to the original HNM,

$$\mathcal{H} = \mathcal{H}_{\mathrm{HN}} + \sum_{x=1}^{L} V\cos(\pi x) n_x. \tag{4}$$

When $h = \Delta = 0$, this term generates a spectrum with two bands separated by a gap of width $2V$. In the non disordered case where $h \neq 0$ and $\Delta = 0$ we obtain the following eigenvalues

$$\epsilon_k = \pm\frac{t}{2}\sqrt{4V^2/t^2 + 2 + e^{2h+ik\,2\pi/L} + e^{-2h-ik\,2\pi/L}} \tag{5}$$

with $k = 1, 2 \ldots L/2$. In this ordered case, the spectrum has a gap if $V > V_{\mathrm{c}}^{\mathrm{o}} = t\sinh(h)$ and its width W_{G} is given by

$$W_{\mathrm{G}} = 2\sqrt{V^2 - t^2\sinh^2(h)}. \tag{6}$$

Even when $\Delta = 0$, there is a transition in this model corresponding to the opening of the gap at half-filling (see Fig. 4). The gap opens with exponent $\beta = 1/2$ since near the transition $W_{\mathrm{G}} \simeq \sqrt{2V_{\mathrm{c}}^{\mathrm{o}}(V - V_{\mathrm{c}}^{\mathrm{o}})}$.

3 Phase diagram

In the presence of both disorder and the periodic potential, the spectrum of the model can show several different topologies. We calculate the eigenspectrum for one disorder realisation of a large size system ($L = 1000$) and analyse the different topologies appearing. We checked that these topologies were still present for other sizes ($L = 500, L = 2000$) and other disorder realisations.

Scanning horizontally along the real axis in the complex eigenvalue plane, we observe three types of regions in the spectrum. First we observe cases of real eigenvalues corresponding to localized (L) states. Second we observe regions with complex eigenvalues corresponding to extended (E) states. Finally we observe some gaps (G) in the spectrum. A given topology is characterized by the succession of these different regions as one increases the real part of the eigenvalue, $\mathrm{Re}(\epsilon_k)$. The different topologies we observed are shown in Figure 5 and their position in the (V, Δ) plane for a fixed value $h = 0.6$ is shown in Figure 6. As an example, the phase shown in Figure 5a is denoted as the LEL phase since we observe a central region of extended states (E) between two regions of localized states (L) with no gaps.

The location of these different phases for $h = 0.6$ is shown in Figure 6 for a given realization. As expected, a gap appears for V large enough. For moderate disorder ($\Delta < 2$), the opening of the gap happens approximately at the same value $V_{\mathrm{c}}^{\mathrm{o}} = \sinh 0.6 = 0.636$ as in the ordered, $\Delta = 0$ case. Upon increasing Δ, the original low disorder E and EGE phases are modified as some of the extended states are transformed into localized ones at the edges of

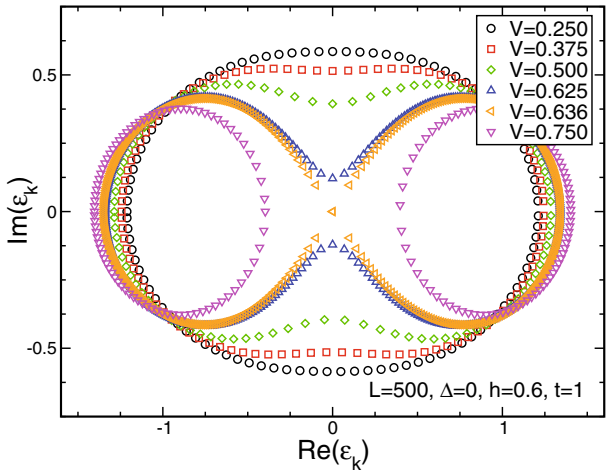

Fig. 4. (Color online) With the periodic potential, a gap is opened for $V > V_c^o = t\sinh(h)$ although all the states remain extended. $V_c^o \simeq 0.636$ in the case shown, $t = 1.0, h = 0.6$.

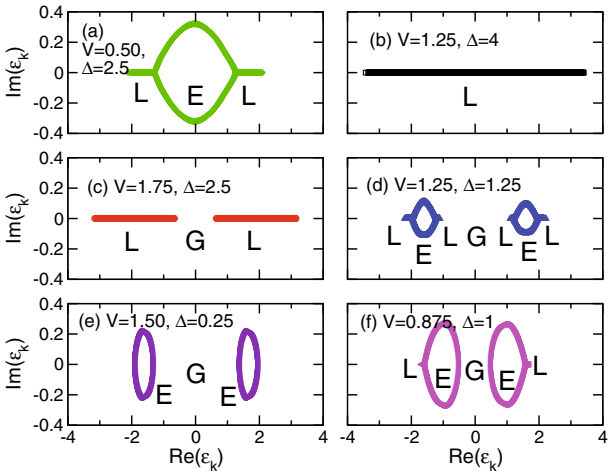

Fig. 5. (Color online) Different topologies of the eigenspectrum for one realization of a $L = 1000$ system and for $h = 0.6$. The simple E topology (only extended states without a gap) and the rarely observed LELEL are not shown. See text for discussion.

the extended regions, leading to the LEL and LELGLEL (or LEGEL) phases respectively. In the LEGEL phase, localization first appears on the external edge of the extended regions and not on the border of the gap. This is consistent with the fact that localized states appear first for the extremal eigenvalues in the Anderson model.

In a very small region of the phase space, we also observe a LELEL phase where the region between the two extended blobs is filled by localized states but no gap appears. As Δ is increased further, all the extended states disappear leading to the large disorder L and LGL phases. When V and Δ are both large, the transition from the L phase to the LGL phase occurs at $V_c = \Delta/2$ which is the result expected in the one site limit, when the hopping terms are neglected. In the one site limit the gap opens like $W_G \simeq 2(V - V_c)$ which is a different behavior from the opening of the gap due to the periodic potential.

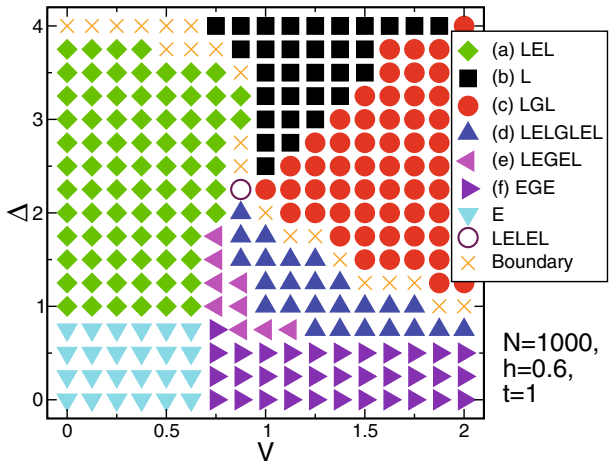

Fig. 6. (Color online) The different phases observed in the Hatano-Nelson model for a given realization on a $L = 1000$ system size and for $t = 1, h = 0.6$. At the boundary between different phases, the behavior is sometimes irregular for a finite size system and does not fall into one of the identified categories. The labels (a)−(f) correspond to the cases shown in Figure 5.

For a given realisation, close to the boundary between two phases, the spectrum becomes disordered and it is difficult to classify it as belonging to one of the simple topologies identified before. These regions are indicated by "×" in the chosen example (Fig. 6). To calculate more precisely the boundaries between the different phases, it is then necessary to use different quantitative indicators and to average those over several disorder realisations. First we measure the width of the gap in the system and determine whether it is present or not. Second we determine if the spectrum is made of complex values (extended states) only, of a mixture of complex and real values (extended and localized states), or of real values only. We consider a $L = 1000$ system and average over 10 realisations. Drawing these three lines in the phase space, we obtain the phase diagram shown in Figure 7. With these quantities, we cannot distinguish the LELGLEL from the LEGEL phases, as well as the LELEL from the LEL phase.

We observe an interesting reentrant behavior. If the system is in the EGE phase but the gap is not too large, when we increase Δ, the gap will be closed by the disorder but the states in the middle of the spectrum will remain extended (Fig. 8). Then we observe a transition where increasing disorder drives the gapped system into an ungapped phase. This can be understood as follows: as the disorder is increased, the E regions have a tendency to flatten out as they evolves towards L regions with only real values. By doing so, the E regions spread along the real axis. If the gap is not to large, two gapped E regions can then merge in the process, which is happening here.

In the Hermitian $h = 0$ phase diagram, one excepts extended states only for $\Delta = 0$ as any amount of disorder should localized states in a one dimensional system. Hence there should be only two phases in finite regions of the phase diagram: the L and LGL phases and the transition

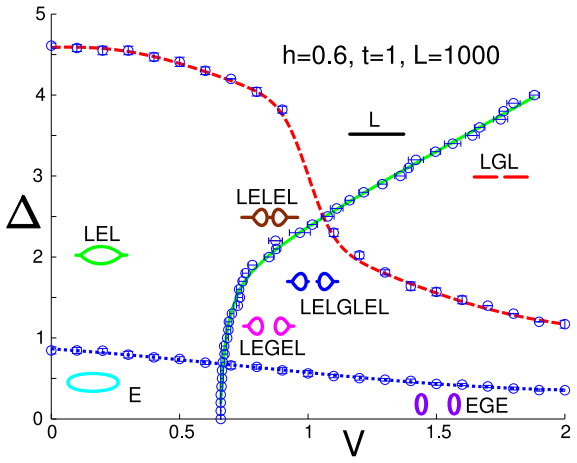

Fig. 7. (Color online) The phase diagram obtained by averaging several disorder realisations to calculate the boundary between different regions. The smooth lines are fits to the data. The continuous green line marks the limit between gapped and ungapped regions. The dotted blue, the limit between a spectrum without any real values and a spectrum with real and complex values. The dashed red line is the limit between a spectrum with real and complex eigenvalues and a spectrum with only real values. The different phases are characterized by the different types of spectrum that are sketched in the figure. These different phases are labelled by a succession of letters corresponding to the different types of states that appear in the spectrum as the real part of the eigenvalues is increased: localized states (L) corresponding to real eigenvalues, extended states (E) corresponding to complex eigenvalues and gaps (G).

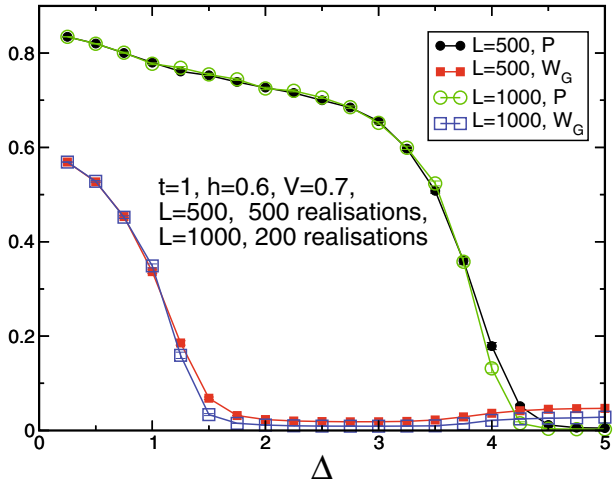

Fig. 8. (Color online) For $V = 0.7$, upon increasing the disorder, the gap W_G is closed before the states becomes localised, which is shown by the participation ratio P becoming zero. Here, the quantities are averaged over only 5% of the total number of eigenstates located in the middle of the spectrum, to get rid of possible bias induced by states located at the edges of the spectrum. The measurements show the crossings of the two boundaries of the phase diagram at largest Δ (gap closing and all extended states vanishing) for $V = 0.7$ in Figure 7, but not the crossing of the boundary at smallest Δ when localized states first appear.

between those two phases should happen for $\Delta \simeq 2V$. The E phase should appear only for $\Delta = V = 0$ and the EGE phase only for $V = 0$. The phase diagram is then deeply modified by the addition of the non hermitian term $h \neq 0$ as the existence of extended states is expanded to a whole range of the (Δ, V) plane.

4 Transitions

4.1 Opening of the gap

As expected, we observe two different behaviors for the opening of the gap for a fixed value of Δ as V is increased (see Fig. 9). If $\delta = V - V_c$, we have a behavior $W_G \propto \sqrt{\delta}$ as in the non interacting regime, whereas $W_G \propto \delta$ in the strongly disordered regime Figure 9. The transition between those two different behaviors happens precisely at the point where, in the phase diagram Figure 7, we are passing from the low disorder into the large disorder regime. For $\Delta < 2$, the transition almost takes place at the non-interacting critical value V_c^o, the transition occurring at nearly constant V and with the square root behavior. Above this value, the transition takes place approximately at $V_c = \Delta/2$ with the linear behavior, which is characteristic of the disordered regime.

4.2 Finite size analysis of the localization transition

It is possible to analyze more precisely the transition to the localized regime by performing a finite size analysis of the participation ratio. We define the mean participation ratio $P = \sum_k P_k/L$ which becomes zero when we have only localized states. We found that the participation ratio is varying linearly with the size of the system L. In Figure 10 we show the result of a finite size analysis for a given value of V and for different values of Δ. We see that P extrapolates to zero for values larger than $\Delta_c \simeq 2.5$. This is in agreement with the phase diagram obtained with a $L = 1000$ size (Fig. 7).

5 Conclusion

We have studied the Hatano-Nelson model in the presence of a periodic potential. We have determined the phase diagram of the system and shown that it presents a variety of different localized or gapped phases, distinguished by the topology of the eigenspectrum in the complex plane. Interesting insulator-metal transitions can occur, driven by increasing disorder. Finally, we have determined how the gap and participation ratio evolve close to these transitions.

There are some interesting analogies between eigenspectra features induced by a periodic potential, discussed here, and those which appear in crossing over from one to two dimensions [16]. We comment first that the $d = 2$ model can be trivially solved in the clean limit $\Delta = 0$ with

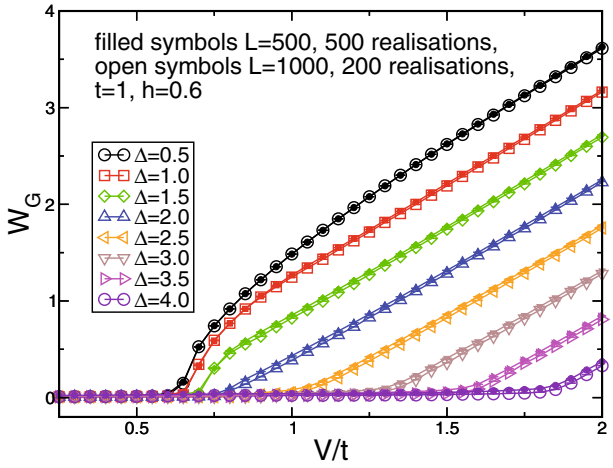

Fig. 9. (Color online) Evolution of the gap as a function of V. For $V < 2.0$, the gap opens like $W_G \propto \sqrt{V - V_c}$ as in the non disordered case. For $V \geq 2.0$, the opening of the gap is linear as expected for a transition in the disorder regime.

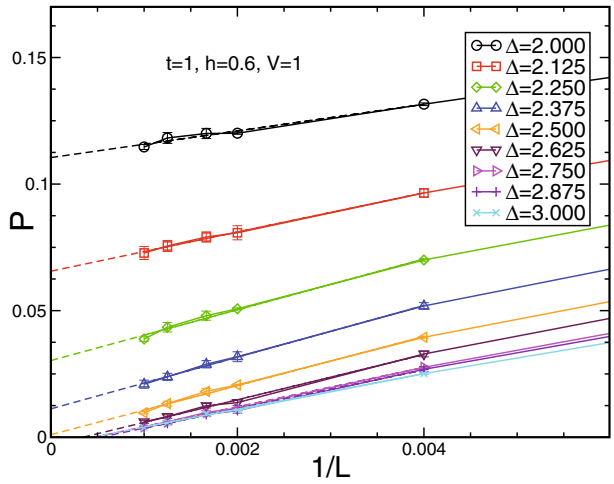

Fig. 10. (Color online) Finite size scaling analysis of the participation ratio. For this value of V, the transition towards localization happens at $\Delta_c \simeq 2.5$.

hoppings t_x, t_y and non-Hermiticity parameters h_x, h_y. In fact, the eigenvalue distribution in the complex plane is obtained by taking ellipses determined by t_y and h_y, and placing them with centers at each of the eigenvalues of equation (2). In the limit of large lattice sizes these eigenvalues become space filling in the complex plane.

However, just as discussed here, different topologies are possible. If t_y and h_y are small compared to t_x and h_x (or vice-versa) one is overlaying small ellipses on a background of a larger ellipse, and the eigenspectrum retains a hole in the origin. When the hoppings in the two dimensions are comparable, in contrast, the central hole can get filled in. It is not surprising that a particularly close analogy is obtained by considering a system consisting of two chains since such a situation describes, as with the periodic potential considered here, a lattice with two different types of sites (two bands). The resulting eigenvalue spectra reflect considerable similarities with those found in this paper. See, for example, Figure 2 of [16].

Random non-Hermitian matrices also arise in the study of quenched quantum chromo-dynamics at finite quark density [17,18]. While the structure of the matrices does not take the precise form of the HNM, it is interesting that in certain cases ("Dyson index" $\beta = 4$) a gap appears in the spectrum in the complex plane, analogous to that found here [18]. That is, the eigenvalue distribution can be driven to zero in a region in the vicinity of the imaginary axis, not unlike the effect of increasing V in Figure 4. (In these studies the spatial dimensionality is greater than one so that the eigenvalues are space filling as opposed to lying along one-dimensional curves). Indeed, a key result [17] is that the appearance of a gap around the imaginary axis requires a finite value of the appropriate tuning parameter, the chemical potential μ, much as our phase diagram (Fig. 6) requires a finite staggered potential $V > V_c \simeq 0.7$ for the appearance of a gap.

The original motivation for the HNM was the problem of flux line motion in type II superconductors. Specifically, deliberate heavy ion irradiation [19] produces random tracks along which the flux lines like to sit, and a transverse magnetic field then provides the 'non-Hermiticity' which attempts to delocalize them. It is also possible to provide regularly patterned pinning centers, which would be a realization of the staggered $\pm V$ term in the extension of the HNM presented here [20–26]. Our phase diagram, Figure 6 indicates that the amount of random disorder Δ required to produce localized phases in general increases with the amplitude V of the patterned potential, so that critical currents would decrease as patterned pinning centers are established if the modulation is at the atomic level. It would be interesting to study the effect of regular variation in the site energy at longer length scales, such as would more typically be accessed in experiments with patterned pinning.

We acknowledge support from the National Science Foundation under award NSF-ITR-013390, the Natural Science Foundation of Shanghai (10ZR1403400), and ARO Award W911NF0710576 with funds from the DARPA OLE Program. This work was also supported by the CNRS-UC Davis EPOCAL LIA joint research grant. The authors would like to thank B. Holly and B. Grémaud for useful input. Z. Bai and R.T. Scalettar wish to thank the hospitality of Fudan University where portions of this work were done.

References

1. P.W. Anderson, Phys. Rev. **109**, 1492 (1958)
2. D.J. Thouless, Phys. Rep. **13**, 93 (1974)
3. J. Billy, V. Josse, Z. Zuo, A. Bernard, B. Hambrecht, P. Lugan, D. Clément, L. Sanchez-Palencia, P. Bouyer, A. Aspect, Nature **453**, 891 (2008)
4. G. Roati, C. D'Errico, L. Fallani, M. Fattori, C. Fort, M. Zaccanti, G. Modugno, M. Modugno, M. Inguscio, Nature **453**, 895 (2008)
5. N. Paris, K. Bouadim, F. Hébert, G.G. Batrouni, R.T. Scalettar, Phys. Rev. Lett. **98**, 046403 (2007)

6. K. Bouadim, N. Paris, F. Hébert, G.G. Batrouni, R.T. Scalettar, Phys. Rev. B **76**, 085112 (2007)
7. E. Abrahams, P.W. Anderson, D.C. Licciardello, T.V. Ramakrishnan, Phys. Rev. Lett. **42**, 673 (1979)
8. P.A. Lee, T.V. Ramakrishnan, Rev. Mod. Phys. **57**, 287 (1985)
9. D. Belitz, T.R. Kirkpatrick, Rev. Mod. Phys. **66**, 261 (1994)
10. N. Hatano, D.R. Nelson, Phys. Rev. Lett. **77**, 570 (1996)
11. N. Hatano, D.R. Nelson, Phys. Rev. B **56**, 8651 (1997)
12. N. Hatano, D.R. Nelson, Phys. Rev. B **58**, 8384 (1998)
13. J. Feinberg, A. Zee, Phys. Rev. E **59**, 6433 (1999)
14. J. Feinberg, A. Zee, Nucl. Phys. B **552**, 599 (1999)
15. P. Le Doussal, unpublished
16. A. Zee, Physica A **254**, 300 (1998)
17. M.A. Stephanov, Phys. Rev. Lett. **76**, 4472 (1996)
18. M.A. Halasz, A.D. Jackson, J.J.M. Verbaarschot, Phys. Rev. D **56**, 5140 (1997)
19. L. Civale, Supercon. Sci. Technol. **10**, 11 (1997)
20. M. Baert, V.V. Metlushko, R. Jonckheere, V.V. Moshchalkov, Y. Bruynseraede, Phys. Rev. Lett. **74**, 3269 (1995)
21. E. Rosseel, M. Van Bael, M. Baert, R. Jonckheere, V.V. Moshchalkov, Y. Bruynseraede, Phys. Rev. B **53**, R2983 (1996)
22. V.V. Moshchalkov, M. Baert, V.V. Metlushko, E. Rosseel, M. Van Bael, K. Temst, R. Jonckheere, Y. Bruynseraede, Phys. Rev. B **54**, 7385 (1996)
23. J.Y. Lin, M. Gurvitch, S.K. Tolpygo, A. Bourdillon, S.Y. Hou, J.M. Phillips, Phys. Rev. B **54**, R12717 (1996)
24. K. Harada, O. Kamimura, H. Kasai, T. Matsuda, A. Tonomura, V.V. Moshchalkov, Science **274**, 1167 (1996)
25. C. Reichhardt, C.J. Olson, J. Groth, S. Field, F. Nori, Phys. Rev. B **53**, R8898 (1996)
26. C. Reichhardt, C.J. Olson, J. Groth, S. Field, F. Nori, Phys. Rev. B **54**, 16108 (1996)